On the Convective and Absolute Nature of Instabilities in Finite Difference Numerical Simulations of Open Flows

C. Cossu and T. Loiseleux

LadHyX, CNRS UMR 7646, École Polytechnique, F-91128 Palaiseau Cedex, France
E-mail: carlo@ladhyx.polytechnique.fr and thomas@ladhyx.polytechnique.fr

In numerical simulations of unstable flows the absolute or convective nature of the instability can be modified by numerical effects. We introduce a convective/absolute analysis of the dispersion relations associated with discretized operators. This analysis leads to conditions on the discretization parameters in order to avoid numerical transition from absolute to convective instability and vice versa. In numerical simulations of non-parallel flows, local numerical transitions, of the kind described in this paper, could lead to the wrong global dynamics.   © 1998 Academic Press

1. INTRODUCTION

In the last ten years the notions of local/global and absolute/convective instabilities have been recognized as essential for understanding the spatio-temporal dynamics of open flows. The concept of absolute and convective instability was originally introduced in plasma physics [1, 2] and has been successfully applied to open flow dynamics [7, 8]. It applies to parallel flows, i.e., flows invariant under translation in the streamwise direction x. The criterion used to discriminate between absolute and convective instability is based on the linear impulse response, i.e., the Green function $G(x, t)$, in the "laboratory" frame, which is the reference frame singled out by boundary conditions. The instability is *absolute* when $G(x, t)$ becomes infinite with time at any fixed location x in the laboratory frame and *convective* when it goes to zero in the laboratory frame (and to infinity in at least one different Galilean frame). In the laboratory frame, a convectively unstable flow will relax everywhere to the basic state as the transient is advected downstream. The flow will behave as a spatial amplifier when spatially localized harmonic forcing is applied. By contrast, in an absolutely unstable flow, a transient will initially grow in place and then saturate, leading to self-sustained oscillations. For spatially evolving flows the global behavior of

the flow can be deduced by a local analysis, i.e., an analysis in which in each point the local parameters are frozen and a parallel flow analysis is developed, if the instability wavelength is small compared to the characteristic inhomogeneity length. Flows that are locally convectively unstable everywhere behave as noise amplifiers while a finite region of local absolute instability is necessary to obtain a global instability leading the flow to an intrinsic oscillatory behavior [4].

The numerical simulation of unsteady flows has become a routine task in many fields of science and technology such as meteorology, plasma physics, or applied aerodynamics. In a numerical simulation, changing the absolute or convective nature of the instability, responsible for the time-dependent behavior, can result in the wrong global dynamics of the flow, for instance a transition from a noise amplifier behavior to an oscillator behavior or vice versa. The problem we analyze in this paper is that the absolute and convective nature of the instability can be modified by numerical effects. This is obvious when one considers that the dispersion relation associated with the physical system is altered by the numerical scheme. It is thus important to ensure that, at least locally, the nature of the instability is not changed by numerical effects. Here we analyze the simplest case in which this phenomenon can be observed, i.e., a finite difference numerical simulation of a parallel one-dimensional unstable flow. This analysis can be extended to non-parallel flows by using the parallel analysis locally just as is done for the von Neumann numerical stability analysis of non-parallel flows. We hope that the techniques we shall explain below will prove useful in much the same way.

The idea of analyzing the dispersion relation of a numerical scheme in order to better understand its properties, such as the numerical group velocity, is not new and a review is given by Trefethen [14]. However, all previous analyses were limited to neutral or stable flows, to real wavenumbers and frequencies, and did not consider the convective or absolute nature of the instabilities. In this paper we consider both stable and unstable dissipative systems, complex frequencies and wavenumbers, and we analyze the dispersion relation associated with the discretized operator to detect the convective or absolute nature of numerical solutions.

The numerical effects we analyse here are not to be confused with the ones induced by numerical boundary conditions. Buell and Huerre [3] showed that global self-sustained oscillations can be observed in numerical simulations of flows that are convectively unstable everywhere and should behave just as noise amplifiers. This spurious global behavior is due to the outflow numerical boundary conditions that create destabilizing pressure feedback loops [3]. By contrast the numerical effects we analyse here appear also in infinite domains and for a model problem that does not allow pressure feedback: they are intrinsic to the numerical discretization.

This paper is organized as follows. In Section 2 we introduce the Ginzburg–Landau equation, used as a model in this paper, and three sample numerical schemes. The dispersion relations associated with the model equation and its discretizations are briefly reviewed in Section 3. In Section 4 we apply the temporal stability and convective/absolute analyses to the considered dispersion relations and discuss them in Section 5. Finally, some conclusions are drawn in Section 6.

2. THE MODEL EQUATION AND ITS DISCRETIZATION

We illustrate our points on the linearized Ginzburg–Landau operator. This is the simplest model that can show convective and absolute instabilities [7]. The Ginzburg–Landau

equation describes the wave amplitude in a bifurcating spatially extended system and has been considered to model the transition of closed [10] as well as open [13] fluid dynamical systems

$$\partial_t A = \mu A - U \partial_x A + \gamma \partial_{xx} A, \tag{1}$$

with U the mean (positive) advection velocity, μ the bifurcation parameter, and γ the (positive) diffusion coefficient. We consider three sample discretizations of Eq. (1). The spatial derivatives are discretized by centered, symmetric second-order formulas in all the schemes. If we define the function $f(x, t) = \mu A - U \partial_x A + \gamma \partial_{xx} A$ we have

$$f_j^n = \mu A_j^n - U \frac{A_{j+1}^n - A_{j-1}^n}{2\Delta x} + \gamma \frac{A_{j+1}^n - 2A_j^n + A_{j-1}^n}{\Delta x^2}, \tag{2}$$

where $A_j^n = A(x_j, t_n)$ and $f_j^n = f(x_j, t_n)$. The grid is equally spaced so that $x_j = j\Delta x$ and $t_n = n\Delta t$. The first scheme (EE) is based on Euler-explicit discretization in time, the second (CN) on a Crank–Nicholson (semi-implicit) discretization, and the third (EI) on an Euler-implicit one.

$$
\begin{aligned}
\frac{A_j^{n+1} - A_j^n}{\Delta t} &= f_j^n && \text{(EE)} \\[2mm]
\frac{A_j^{n+1} - A_j^n}{\Delta t} &= \frac{f_j^{n+1} + f_j^n}{2} && \text{(CN)} \\[2mm]
\frac{A_j^{n+1} - A_j^n}{\Delta t} &= f_j^{n+1} && \text{(EI)}.
\end{aligned}
\tag{3}
$$

The EE and EI schemes are first-order accurate in time, while the CN one in second-order accurate.

3. PHYSICAL AND NUMERICAL DISPERSION RELATIONS

If we consider solutions $A(x, t)$ of Eq. (1) in the form of normal modes $\tilde{A}e^{i(kx - \omega t)}$, where k and ω are the complex spatial wavenumber and temporal frequency respectively, we obtain the *physical dispersion relation*:

$$\omega = Uk + i(\mu - \gamma k^2). \tag{4}$$

In a similar fashion, by considering solutions A_j^n of Eq. (3) in the form of normal modes $\check{A}e^{i(kx_j - \omega t_n)}$, we obtain the corresponding *numerical dispersion relations*,

$$
\begin{aligned}
\frac{e^{-i\omega\Delta t} - 1}{\Delta t} &= F(k; \Delta x, \mu, U, \gamma) && \text{(EE)} \\[2mm]
\frac{-2i \tan \omega\Delta t}{\Delta t} &= F(k; \Delta x, \mu, U, \gamma) && \text{(CN)} \\[2mm]
\frac{1 - e^{i\omega\Delta t}}{\Delta t} &= F(k; \Delta x, \mu, U, \gamma) && \text{(EI)}
\end{aligned}
\tag{5}
$$

with

$$F = \mu - \frac{iU}{\Delta x} \sin k\Delta x + \frac{2\gamma}{\Delta x^2}(\cos k\Delta x - 1). \tag{6}$$

One can immediately verify that for $\Delta x \to 0$ and $\Delta t \to 0$, we recover the physical dispersion relation, Eq. (4), for the three numerical dispersion relations.

It is convenient to introduce the dimensionless variables $\hat{\omega} = \omega\gamma/U^2$, $\hat{k} = k\gamma/U$, and parameters $\hat{\mu} = \mu\gamma/U^2$, $R = \Delta xU/\gamma$, and $S = \Delta tU^2/\gamma$. In the literature on numerical stability analysis the two parameters $\sigma = U\Delta t/\Delta x$ and $\beta = \gamma\Delta t/\Delta x^2$ are usually used. They are related as follows to the parameters that we use in this study: $\sigma = S/R$, $\beta = S/R^2$. The physical dispersion relation, Eq. (4), may then be cast in dimensionless form,

$$\hat{\omega} = \hat{k} + i(\hat{\mu} - \hat{k}^2) \tag{7}$$

as well as the numerical dispersion relations, Eq. (5)

$$\frac{e^{-i\hat{\omega}S} - 1}{S} = \hat{F}(\hat{k}; R, \hat{\mu}) \qquad \text{(EE)}$$

$$\frac{-2i \tan \hat{\omega}S}{S} = \hat{F}(\hat{k}; R, \hat{\mu}) \qquad \text{(CN)} \tag{8}$$

$$\frac{1 - e^{i\hat{\omega}S}}{S} = \hat{F}(\hat{k}; R, \hat{\mu}) \qquad \text{(EI)}$$

with

$$\hat{F} = \hat{\mu} - \frac{i}{R} \sin \hat{k}R + \frac{2}{R^2}(\cos \hat{k}R - 1). \tag{9}$$

4. CONVECTIVE/ABSOLUTE INSTABILITY ANALYSIS

As pointed out in the Introduction, the stable and convectively or absolutely unstable nature of a parallel flow is defined by the behavior of its impulse response $G(x, t)$ but can also be deduced from the analysis of its dispersion relation [1, 2, 7]. A stable flow admits only damped temporal modes, i.e., $\mathcal{I}m[\hat{\omega}(\hat{k})] < 0$ for every real wavenumber $\hat{k}$, otherwise it is unstable. For the physical dispersion relation, Eq. (7), we have a bifurcation from a stable to an unstable behavior for $\hat{\mu} = 0$ with a most amplified wavenumber $\hat{k}_{max} = 0$.

For unstable flows the behavior of the Green's function at a *fixed* (in the laboratory frame) spatial location x is dominated by the *absolute wavenumber* k_0 corresponding to a zero group velocity $d\hat{\omega}/d\hat{k}(\hat{k}_0) = 0$. An observer at x will see the impulse response dominated by the *absolute frequency* $\hat{\omega}_0 = \hat{\omega}(\hat{k}_0)$. If $\mathcal{I}m[\hat{\omega}_0] < 0$ we are in a convectively unstable regime, whereas the instability is absolute if $\mathcal{I}m[\hat{\omega}_0] > 0$. The absolute wavenumber and frequency correspond to a singularity of the dispersion relation that must fulfill a pinching requirement [1]. The determination of the convective or absolute nature of an instability based on the analysis of the singular points of the dispersion relation is known as the Briggs–Bers criterion [1, 2].

For the physical dispersion relation, the complex group velocity is $d\hat{\omega}/d\hat{k} = 1 - 2i\hat{k}$, the absolute wavenumber is $\hat{k}_0 = -i/2$, and the absolute frequency is $\hat{\omega}_0 = i(\hat{\mu} - 1/4)$; the

flow will thus be physically convectively unstable for $0 < \hat{\mu} < 1/4$ and physically absolutely unstable for $\hat{\mu} \geq 1/4$.

We performed an absolute/convective stability analysis of the numerical schemes by using the Briggs–Bers criterion applied to the numerical dispersion relations, Eq. (8). For this analysis, limitations on frequency and wavenumber bandwidths must be introduced due to the numerical discretization: $-\pi/R < \hat{k} < \pi/R$ and $-\pi/S < \hat{\omega} < \pi/S$. While the temporal stability analysis of numerical dispersion relations is fully equivalent to the widely used von Neumann stability analysis, the convective/absolute instability analysis applied to the dispersion relations of numerical schemes is the main novelty that we introduce in this paper. The detailed results of the analysis are reported in Appendix A, and we discuss them, in the following sections, separately for the three numerical schemes we considered. As the spatial discretization is the same for the three schemes, the stability results for $S = 0$ are the same for the three schemes.

4.1. Euler Explicit Scheme

The stability diagrams of the EE scheme are reported in Fig. 1. The physically stable case is considered in Fig. 1a. As it is well known, this scheme produces a numerical instability over much of the (R, S) plane. We found that this numerical instability is absolute in a large region, and convective in a narrow band. The physically neutral case ($\hat{\mu} = 0$), in which the Ginzburg–Landau equation reduces to the convection-diffusion one, is considered in Fig. 1b. The curve which separates the stable from the unstable regions is the classical result of the von Neumann stability analysis (see, for example, [6]). In this case it is found that the absolute instability boundary, found by a local analysis, exactly coincides with the global instability boundary, obtained with the spectral radius criterion, when Dirichlet boundary conditions are enforced [6, 12]. The absolute nature of the instability allows an
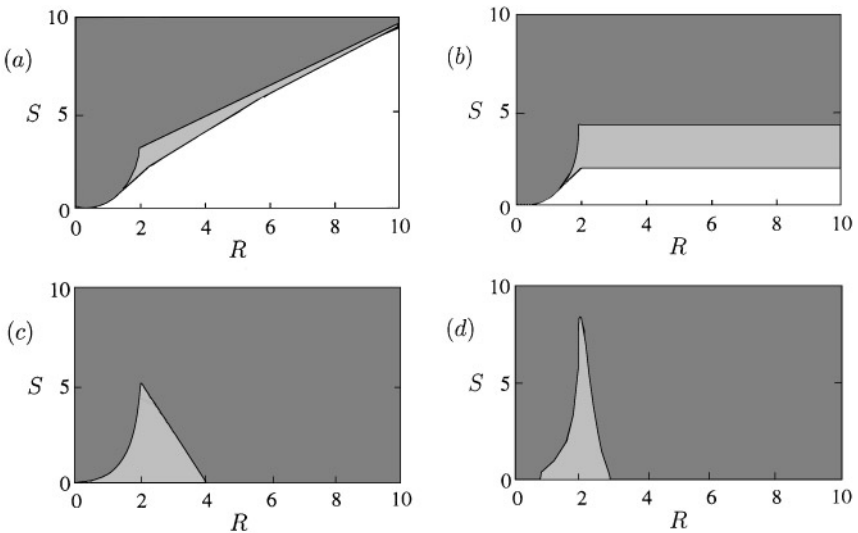

FIG. 1. Stability diagrams for the Euler explicit scheme in (a) a physically stable situation, $\hat{\mu} = -0.125$; (b) a physically neutral situation, $\hat{\mu} = 0$; (c) a physically convectively unstable situation, $\hat{\mu} = 0.125$; and (d) a physically absolutely unstable situation, $\hat{\mu} = 0.26$. The unstable regions are depicted in gray, light gray for a convective instability, and dark gray for an absolute one.

amplified energy radiation from the downstream boundary into the computational domain and thus a global instability. In our view, the concepts of absolute and convective instability applied to numerical schemes should probably permit the extension of the analysis of Trefethen [15], who treated the instability of difference models for hyperbolic initial boundary value problems, to non-hyperbolic and/or unstable systems. This extension is currently under consideration. A physically convectively unstable situation is considered in Fig. 1c. Here, the EE scheme could produce numerically absolutely unstable solutions in a large region of the R, S plane. A physically absolutely unstable situation is considered in Fig. 1d where, if $\hat{\mu} < 1/2$ (less than twice the physical absolute transition critical value) a convective instability could be diagnosed even for small S in a large range of R values.

To ensure numerical stability, even in physically unstable situations, the stability conditions of the physically neutral case are usually enforced. For the EE scheme this corresponds to the limitation $S < R^2/2$ for $R < 2$. In the convectively unstable regime, the limitations on S to avoid transition to a numerical absolute instability are less stringent than the stability condition when $R < 2$. In the absolute instability regime, however, only a limitation on R is necessary to avoid a transition to a numerical convective instability.

4.2. Crank–Nicholson Scheme

As it is well known, this scheme is always numerically stable when the solution is physically stable so we discuss only the physically unstable regime. A physically convectively unstable situation is considered in Fig. 2a where the scheme could produce numerical solutions that are absolutely unstable for every S if a too coarse spatial discretization is chosen (large R). A physically absolutely unstable situation is considered in Fig. 2b where a convectively unstable numerical solution could be observed for every time step in a given range of R. We observe that only the first band (the left one) of absolute instability is the "good" one as the second one (the one on the right) is an absolute instability with a wrong absolute wavenumber. An interesting feature of the CN scheme is that the stability and absolute instability boundaries do not depend on S but only on R: convergence tests based only on time step refinements could leave the convergence path always in the wrong region.

4.3. Euler Implicit Scheme

We report in Fig. 3 the stability diagrams of the EI scheme in the R, S plane. As for the CN scheme we discuss only the physically unstable regime as the scheme is numerically stable in the physically stable regime. A physically convectively unstable case is considered
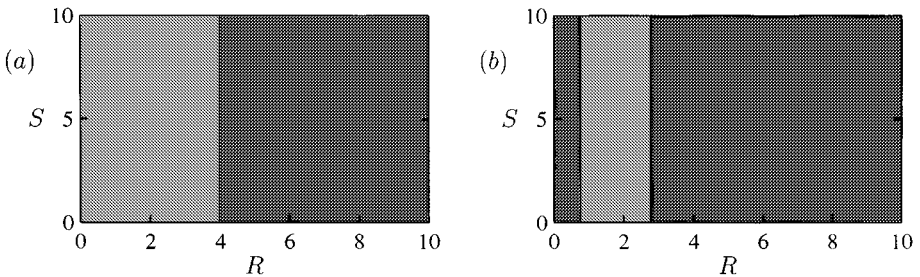

FIG. 2. Stability diagrams for the Crank–Nicholson scheme in (a) a physically convectively unstable situation, $\hat{\mu} = 0.125$; and (b) a physically absolutely unstable situation, $\hat{\mu} = 0.26$. The unstable regions are depicted in gray, light gray for a convective instability, and dark gray for an absolute one.

FIG. 3. Stability diagrams for the Euler implicit scheme in (a) a physically convectively unstable situation, $\hat{\mu} = 0.125$, and (b) a physically absolutely unstable situation, $\hat{\mu} = 0.26$. The unstable regions are depicted in gray, light gray for a convective instability, and dark gray for an absolute one.
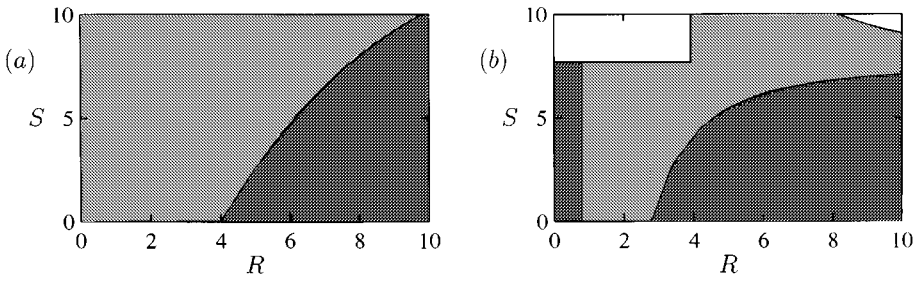
in Fig. 3a, where a region of numerical absolute instability is detectable for large values of R. In that region, for instance, convergence tests based only on time step reductions would always be contained in the wrong region. A physically absolutely unstable situation is considered in Fig. 3b. The region of numerical stabilization increases when $\hat{\mu}$ is increased and the numerically convectively unstable region is reduced. In contrast to the behavior observed for the explicit scheme, the numerical stabilization need not be preceded by a change from absolute to convective instability.

5. DISCUSSION

To verify the results obtained in Section 4, numerical tests have been performed. The three schemes considered were implemented using the homogeneous Dirichlet boundary condition at $x = -L/4$ and $x = 3L/4$. In order to detect the absolute or convective nature of the numerical solution we analyzed the evolution of the "discretized Green function," i.e., the evolution of an initial condition having a value of 1 for $x = 0$ and zero everywhere else. According to the definition, given in Section 1, the instability is convective if, for sufficiently large n, $|G(0, t_n)|$ decreases and is absolute if it increases. The numerical results were obtained with $U = 1$, $\gamma = 1$, $L = 640$ and, to avoid finite domain effects, the runs were stopped before the wavepacket could reach the boundaries of the computational domain. The numerical results, obtained for some sample point in the (R, S) parameter space, confirmed the predictions we developed in Section 4. We found remarkable how easily results affected from numerical transitions could be confused with physically correct results.

For open spatially evolving flows it is believed that the global dynamics can be quali-tatively explained from the nature of the local stability characteristics, i.e., the absolute or convective nature of the instability of the parallel flows associated with the velocity profiles of each streamwise section [7]. For a global instability leading to self-sustained oscillations a finite region of absolute instability is necessary [4, 5], whereas flows that are everywhere locally convectively unstable behave as noise amplifiers [7].

Just as in the physical situation, numerical transitions from local convective instability to local absolute instability, in some regions of the computational domain, could affect the qualitative global behavior of the numerical solution for simulations of even complex spatially evolving flows. On one hand, in a flow that is physically locally convectively unstable everywhere and thus behaves as a noise amplifier, the existence of a finite region of local numerical absolute instability could lead to spurious self sustained oscillations; on the other hand, a numerical transition from local absolute to local convective instability could lead to the numerical suppression of global instabilities.

For flows that experience "physically" a global instability, local transitions can lead to an underestimation or an overestimation of the critical value of the bifurcation parameter. For instance, the onset of the von Kármán vortex street in the circular cylinder wake is produced by a global Hopf bifurcation and is due to the presence of a finite region of local absolute instability in the near wake [9]. In this case, the size of the local absolute instability region can be modified by the numerical effects we described. If the numerical scheme promotes transitions from local convective to local absolute instability the region of numerical absolute instability is larger than the physical one and the critical Reynolds number for the global instability is underestimated. If, on the contrary, transitions from local absolute instability to local convective instability are promoted by numerical effects, the numerical absolute instability region is smaller than the physical one and thus the critical Reynolds number will be overestimated. Such numerical effects could explain the large scatter (between 45 and 54) of critical Reynolds numbers obtained, from numerical simulations, for the circular cylinder wake.

It is already well known that boundary conditions enforced on the boundaries of the computational domain may also affect the global dynamics of the simulated flow. Buell and Huerre [3] showed that destabilizing pressure feedback loops can be generated by the influence of outflow numerical boundary conditions on the upstream boundary, leading flows that are convectively unstable everywhere to spurious global self-sustained oscillations. It is important to stress that the numerical effects we analyse here, in contrast to numerical effects of the type described in [3], appear also in infinite domains and for a model problem that does not allow pressure feedback: they are intrinsic to the numerical discretization just as the numerical instabilities analyzed with von Neumann stability analyses. The point to be retained is that even if one enforces correctly the outflow boundary conditions and the von Neumann stability conditions are satisfied a wrong behavior of the flow may be still induced by numerical transitions from convective to absolute instability and vice versa.

It should also be remarked that the region of the computational plane near the origin is not the only interesting one. Large values of the spatial step Δx, and thus of the parameter R, may be attained for instance in meteorological applications such as global circulation simulations or, in general, in large eddy simulations of turbulent flows. Over a large range of R it may be seen from the results presented in the previous section that a wrong behavior may be maintained even as $S \to 0$. In our sample discretizations we considered only centered schemes for spatial discretizations and perhaps these S-independent numerical transitions for large values R may be avoided by using others spatial discretization schemes.

6. CONCLUSIONS

In this article we showed that in numerical simulations of unstable flows the convective or absolute nature of a physical instability can be modified by numerical effects. Standard convergence tests in the Δx, Δt plane are not sufficient to avoid erroneous behavior of the solution because the convergence path could be contained in the wrong region.

The Briggs–Bers criterion, widely applied to physical dispersion relations to determine the absolute or convective nature of an instability for a continuous operator, is here applied to dispersion relations associated with discretized operators. This type of investigation reveals the impact of the numerical effects on the absolute/convective nature of the instabilities in the numerical solution and allows for the design of appropriate convergence paths in the Δx, Δt plane. It is found that some limitations in the time step Δt and/or in the mesh spacing

Δx are necessary to avoid numerical transitions from convective to absolute instabilities and conversely. For the model equation considered, namely the Ginzburg–Landau equation, three sample discretizations were considered: an Euler-explicit, a Crank–Nicholson, and an Euler-implicit one. For none of these discretizations the numerical stability requirements, given by a von Neumann stability analysis, automatically avoid a wrong convective/absolute behavior of the numerical solution. Numerical simulations validated the predictions derived from the analysis of numerical dispersion relations.

Our analysis has been developed for parallel flows of infinite extent where the theory exactly applies just as the classical von Neumann stability analysis. However, even if it strictly applies to parallel flows, a local von Neumann analysis, and the numerical stability conditions deriving from it, are commonly used to avoid numerical instability in simulations of spatially evolving flows (see for instance [11]). In the same spirit, we suggest using our analysis and criteria as local ones, to ensure that the local nature of the instability, and eventually the global dynamics of the flow, are not altered by the numerical scheme.

APPENDIX A: NUMERICAL STABILITY AND CONVECTIVE/ABSOLUTE INSTABILITY BOUNDARIES

A.1. *Conditions for Temporal Instability*

For $\hat{\mu} \leq 0$ (physically stable situation):

	$0 \leq R \leq 2$	$R \geq 2$
EE	$S > \frac{2R^2}{4 - \hat{\mu} R^2}$	$S > \frac{2 - \hat{\mu} R^2 + \sqrt{\hat{\mu}^2 R^4 - 4\hat{\mu}^2 R^2 - 4\hat{\mu} R^2 + 16\hat{\mu}}}{\hat{\mu}^2 R^2 - 4\hat{\mu} + 1}$
CN	Never unstable	Never unstable
EI	Never unstable	Never unstable

For $\hat{\mu} > 0$ (physically unstable situation):

	$0 \leq R \leq \frac{2}{\sqrt{\hat{\mu}}}$	$R \geq \frac{2}{\sqrt{\hat{\mu}}}$
EE	$\forall S$	$\forall S$
CN	$\forall S$	$\forall S$
EI	$S < 2/\hat{\mu}$	$S < \frac{2R^2}{\hat{\mu}^2 R^2 - 4}$

A.2. *Conditions for Absolute Instability (AI)*

For $\hat{\mu} < 0$ (physically stable situation):

	$0 \leq R \leq 2$	$R \geq 2$
EE	$S > \frac{2R^2}{2 - \hat{\mu} R^2 + \sqrt{4 - R^2}}$	$S > \frac{4 - 2\hat{\mu}^2 R^2}{\hat{\mu}^2 R^2 - 4\hat{\mu} + 1}$
CN	Stable	Stable
EI	Stable	Stable

For $0 < \hat{\mu} < 0.25$ (physically convectively unstable situation):

	$0 \leq R \leq 2$	$2 \leq R \leq \sqrt{\frac{2}{\hat{\mu}}}$	$R \geq \sqrt{\frac{2}{\hat{\mu}}}$
EE	$S > \frac{2R^2}{2 - \hat{\mu}R^2 + \sqrt{4 - R^2}}$	$S > \frac{4 - 2\hat{\mu}R^2}{\hat{\mu}^2 R^2 - 4\hat{\mu} + 1}$	$S > \frac{4 - 2\hat{\mu}R^2}{\hat{\mu}^2 R^2 - 4\hat{\mu} + 1}$
CN	Never AI	Never AI	$\forall S$
EI	$S < 2\frac{\hat{\mu}R^2 - 2}{\hat{\mu}^2 R^2 - 4\hat{\mu} + 1}$	$S < 2\frac{\hat{\mu}R^2 - 2}{\hat{\mu}^2 R^2 - 4\hat{\mu} + 1}$	$S < 2\frac{\hat{\mu}R^2 - 2}{\hat{\mu}^2 R^2 - 4\hat{\mu} + 1}$

For $0.25 < \hat{\mu} < 0.5$ (physically absolutely unstable situation):

	$0 \leq R \leq \sqrt{\frac{4\hat{\mu} - 1}{\hat{\mu}^2}}$	$\sqrt{\frac{4\hat{\mu} - 1}{\hat{\mu}^2}} \leq R \leq 2$	$2 \leq R \leq \sqrt{\frac{2}{\hat{\mu}}}$	$R \geq \sqrt{\frac{2}{\hat{\mu}}}$
EE	$\forall S$	$S > \frac{2R^2}{2 - \hat{\mu}R^2 + \sqrt{4 - R^2}}$	$S > \frac{4 - 2\hat{\mu}R^2}{\hat{\mu}^2 R^2 - 4\hat{\mu} + 1}$	$S > \frac{4 - 2\hat{\mu}R^2}{\hat{\mu}^2 R^2 - 4\hat{\mu} + 1}$
CN	$\forall S$	Never AI	Never AI	$\forall S$
EI	$\forall S$	$S < 2\frac{\hat{\mu}R^2 - 2}{\hat{\mu}^2 R^2 - 4\hat{\mu} + 1}$	$S < 2\frac{\hat{\mu}R^2 - 2}{\hat{\mu}^2 R^2 - 4\hat{\mu} + 1}$	$S < 2\frac{\hat{\mu}R^2 - 2}{\hat{\mu}^2 R^2 - 4\hat{\mu} + 1}$

For $\hat{\mu} > 0.5$ (physically absolutely unstable situation):

	$\forall R$
EE	$\forall S$
CN	$\forall S$
EI	$S < 2\frac{\hat{\mu}^2 R^2 - 2}{\hat{\mu}^2 R^2 - 4\hat{\mu} + 1}$

ACKNOWLEDGMENTS

REFERENCES

1. A. Bers, Linear waves and instabilities, in *Physique des Plasmas*, edited by C. De Witt and J. Peyraud (Gordon & Breach, New York, 1975), pp. 117–225.

2. R. J. Briggs, *Electron-Stream Interaction with Plasma* (MIT Press, Cambridge, MA, 1964).

3. J. C. Buell and P. Huerre, *Inflow/Outflow Boundary Conditions and Global Dynamics of Spatial Mixing Layers*, Report CTR-S88, Center for Turbulence Research, Stanford, CA, 1988.

4. J. M. Chomaz, P. Huerre, and L. G. Redekopp, Bifurcations to local and global modes in spatially developing flows, *Phys. Rev. Lett.* **60**, 25 (1988).

5. R. J. Deissler, Noise-sustained structure, intermittency and the Ginzburg–Landau equation, *J. Statist. Phys.* **40**, 371 (1985).

6. C. Hirsch, *Numerical Computation of Internal and External Flows* (Wiley, New York, 1988).

7. P. Huerre and P. A. Monkewitz, Local and global instabilities in spatially developing flows, *Ann. Rev. Fluid Mech.* **22**, 473 (1990).

8. L. D. Landau and E. M. Lifshitz, Mécanique des fluides, in *Physique Theorique* (MIR, Moscow, 1989), Vol. VI, French edition.

9. P. A. Monkewitz, The absolute and convective nature of instability in two-dimensional wakes at low Reynolds numbers, *Phys. Fluids* **31**(5), 999 (1988).

10. A. C. Newell and J. A. Whitehead, Finite bandwidth, finite amplitude convection, *J. Fluid Mech.* **38**, 279 (1969).

11. R. D. Richtmyer and K. W. Morton, *Difference Methods for Initial Value Problems* (Wiley, New York, 1967).

12. J. L. Siemieniuch and I. Gladwell, Analysis of explicit difference methods for a diffusion-convection equation, *Int. J. Numer. Methods Eng.* **12**, 899 (1978).

13. K. Stewartson and J. T. Stuart, A nonlinear instability theory for a wave system in plane Poiseuille flow, *J. Fluid Mech.* **48**, 529 (1972).

14. L. N. Trefethen, Group velocity in finite difference schemes, *SIAM Rev.* **24**(2), 113 (1982).

15. L. N. Trefethen, Instability of difference models for hyperbolic initial boundary value problems, *Comm. Pure Appl. Math.* **37**(2), 329 (1984).